



## Efficient CO<sub>2</sub> capture by non-aqueous imide/ethylene glycol solvent

Yong Pan <sup>a,b,\*</sup>, Wei Huang <sup>a,b</sup>, QiaoQiao Tang <sup>a,b</sup>, Bo Sun <sup>c,\*</sup>, Dengyi Ma <sup>d</sup>, BaoMing Xu <sup>a,b</sup>

<sup>a</sup> Hubei Provincial Key Laboratory of Green Materials for Light Industry, Hubei University of Technology, Wuhan 430068, China

<sup>b</sup> Collaborative Innovation Center of Green Light Weight Materials and Processing, Hubei University of Technology, Wuhan 430068, China

<sup>c</sup> Shandong Zhongsheng Pharmaceutical Equipment Co., Ltd, Yantai, Shandong Province 264010, PR China

<sup>d</sup> China Mobile Group Hubei Co., Ltd, Wuhan 430023, China



### ARTICLE INFO

#### Keywords:

CO<sub>2</sub> capture

Succinimide

Ethylene glycol

Imide-based bases

### ABSTRACT

Man-made CO<sub>2</sub> emissions give rise to an important influence on climate and human survival, which has attracted widespread attention. Traditional absorbents such as aqueous amines used for CO<sub>2</sub> capture often suffer from high regeneration energy and corrosiveness. In this regard, non-aqueous amine solutions have high energy-saving potential because organics have lower vaporization enthalpy and heat capacity than water. Herein, we explored the potential absorbent composed of ethylene glycol and imide-based bases to capture CO<sub>2</sub>. The CO<sub>2</sub> uptake in imide-based ethylene glycol absorbent was studied, experimental results showed that succinimide/glycol-20 wt% have the highest CO<sub>2</sub> solubility, and still maintains a high absorption capacity after 8 regeneration cycles. And the absorption mechanism has been confirmed the possible intermolecular hydrogen bonding and van der Waals forces between carbon dioxide and succinimide molecules through molecular simulation. The regeneration energy consumption is only 2.243 GJ/t CO<sub>2</sub> through process simulation calculation, which is lower than the conventional absorbent, further indicating that the fabricated absorbent have exhibits the large potential to absorb CO<sub>2</sub> from flue gas.

### 1. Introduction

It is widely believed that man-made carbon dioxide emissions from industrial activities are the main reason for the global climate change, and reducing CO<sub>2</sub> emissions has become a consensus among countries [1]. Carbon capture, utilization, and storage (CCUS) are the main technological means for large-scale low-carbon utilization of fossil fuels, and also an important support for promoting economic and social development, energy security [2,3]. Among the existing capture approaches, such as adsorption [4], low-temperature fractionation [5], membrane separations [6], physical or chemical-solvent absorption [7–9].

At presently, a 30 wt% of monoethanolamine (MEA) aqueous solution is considered a reference absorbent. However, the severe degradation of amines at high temperatures and large energy consumption are the major obstacles hindering the large-scale application of aqueous amine technology [10,11]. Usually, absorbent regeneration require a high energy consumption, accounting for approximately 60–80 % of the whole CO<sub>2</sub> captured by aqueous amines [11,12]. It has been clearly noted that the use of water as a solvent is the biggest drawback in terms of energy consumption for the regeneration of aqueous amine

absorbents, due to the high specific heat capacity and evaporation enthalpy of the water solvent, as well as the high desorption temperature of 100–120 °C [13,14]. Therefore, researchers have invested a lot of effort in developing new absorbents for energy-saving processes, and the biggest challenge in this field is to maintain the relative capture performance with water-based amines, at least to some extent avoiding the main drawbacks of high regeneration energy.

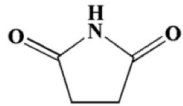
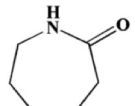
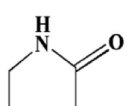
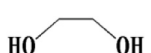
It has been proven that using organic solvents instead of water in absorbents has remarkable advantages, potentially reducing corrosiveness, saving regeneration energy and degradability [15,16]. In recent years, there has been significant development in non-aqueous absorbents that combine amines with organic compounds, many alkanolamines including MEA [17,18], N-methyldiethanolamine (MDEA) [19,20], 2-amino-2-methyl-1-propanol (AMP) [21–23], 2-(2-aminoethoxy) ethanol (DGA) [24] and diisopropanolamine (DIPA) [25] have been mixed with organic solvents to absorb CO<sub>2</sub>. The reported organic solvents typically include low-volatile alcohols and glycols (such as benzyl alcohol), volatile alcohols (such as methanol, ethanol), or their mixtures, glymes, dimethyl formamide (DMF), and ionic liquids or deep eutectic solvent. However, high-volatile alcohols (such as methanol and ethanol) as co-solvents can cause significant solvent loss when dealing

\* Correspondence to: School of Materials and Chemical Engineering, Hubei University of Technology, Wuhan 430205, China.

E-mail addresses: [m13051792239@163.com](mailto:m13051792239@163.com) (Y. Pan), [sunbo\\_yantai@126.com](mailto:sunbo_yantai@126.com) (B. Sun).

**Table 1**

The chemicals used in this study together with their purity, chemical structure.

Chemical	Abbreviation	Purity (%)	Chemical structure
Succinimide	SC	99.9	
Caprolactam	CA	99.9	
2-pyrrolidone	PY	99.9	
Ethylene glycol	EG	99.5	
CO <sub>2</sub>	—	>99.9	—

**Table 2**

Information of the prepared absorbent used in this study.

Imide	Imide (wt%)	EG(wt%)	Solution abbreviation
SC	20	80	SC/EG-20 wt%
	15	85	SC/EG-15 wt%
	10	90	SC/EG-10 wt%
	5	95	SC/EG-5 wt%
	0	100	EG
CA	20	80	CA/EG-20 wt%
PY	20	80	PY/EG-20 wt%

with large-scale flue gas. Therefore, it was impracticable for industrial applications [26,27]. The DMF solvent may also undergo serious degradation under alkaline conditions, especially at high temperatures. Although the vapor pressure of ionic liquids can be negligible, the low diffusion rate of mass transfer and rapid increase in viscosity also may lead to poor CO<sub>2</sub> capture performance [28,29].

Ethylene glycol (EG) is an important industrial solvent because of its excellent properties such as low melting point, low viscosity, low toxicity, high chemical stability and low vapor pressure, which can be used to clean the exhaust and airflow of industrial production equipment [30]. Meanwhile, EG presents native hydrogen bonding sites so that the potential desorption characters are presented in the regenerative processes of decarbonization solutions dissolving CO<sub>2</sub>. Therefore, EG is chosen as an auxiliary solvent when considering the non-aqueous amine solution. In this study, we designed non-aqueous imide-based absorbents using EG instead of water as a solvent to capture CO<sub>2</sub>. The carbon dioxide capacity of three types of imide/EG systems was systematically evaluated, and absorption thermodynamics and kinetics were also investigated. Meanwhile, the influences of temperature, mass fraction ratio and regeneration were studied. In addition, the CO<sub>2</sub> absorption mechanism was discussed by IR spectroscopy, NMR spectroscopy and molecular simulation.

## 2. Materials and methods

### 2.1. Materials

CO<sub>2</sub> with a mole fraction of 0.99999 is supplied by Hubei Xiangyun Gas Co., Ltd., China. For the preparation of adsorbent, Ethylene glycol (Aldrich), Succinimide (Aldrich), Caprolactam (Aldrich) and 2-pyrrolidone (Aldrich), are used. The information about the involved materials is tabulated in Table 1. All chemicals were obtained in the highest purity grade possible and used as received unless otherwise stated.

### 2.2. Preparation of the absorbents

Succinimide and EG were added into a glass vial (100 mL) at required molar ratio. Then, the vial was heated at 80 °C and the mixture in the vial was stirred until a homogenous solution was formed. Finally, the liquid absorbent can be obtained after the solution was cooled down to room temperature. The samples are presented in Table 2.

### 2.3. CO<sub>2</sub> absorption and desorption experiments

The vapor-liquid equilibrium experiments were conducted in an equilibrium cell to measure the apparent solubility of CO<sub>2</sub> in the

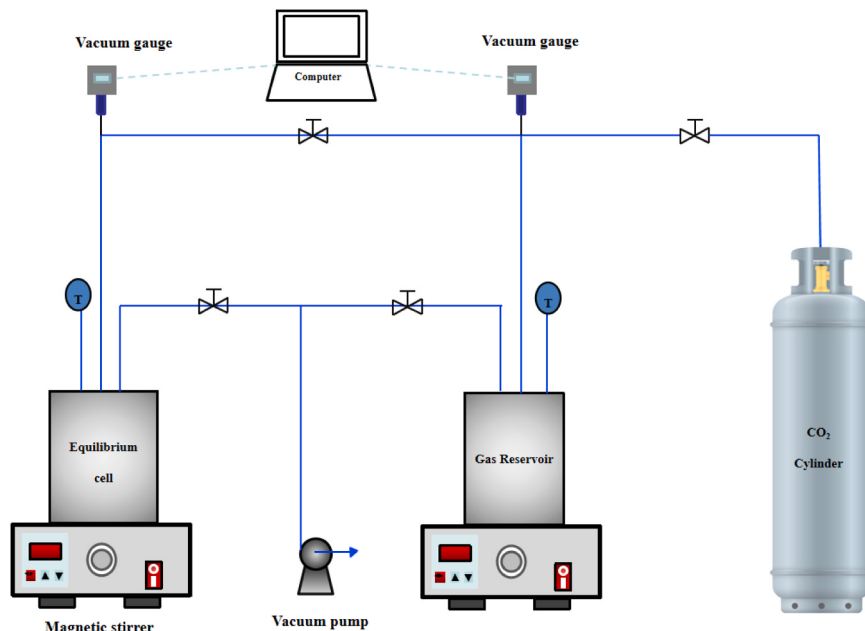


Fig. 1. Process flow diagram for the vapor-liquid equilibrium system.

**Table 3**

Flue gas composition and condition used in this work.

Temperature (K)	298.2
Pressure (kPa)	101.3
Flow rate (kmol/h)	1000
Composition	Mole fraction
CO <sub>2</sub> mole fraction	0.15
N <sub>2</sub> mole fraction	0.85

absorbent. The experimental apparatus of CO<sub>2</sub> absorption for the vapor-liquid equilibrium is presented in Fig. 1. A detailed introduction on experimental procedures can be seen in our previous papers [31,32]. The main parts of the apparatus included a equilibrium cell and a gas reservoir cell, which are both installed in an oil bath. The effective volumes of the equilibrium cell and the gas reservoir cell are 125 cm<sup>3</sup> and 144 cm<sup>3</sup>, respectively. The designed maximum working pressures of these two cells are 10 MPa. The pressure changes of these two cells were recorded and displayed by a computer as a function of the absorption time.

In this study, the amount of CO<sub>2</sub> absorbed in the liquid absorbent was calculated based on the mass balance. The total number of moles of CO<sub>2</sub> ( $n_t$ ) that were injected into the equilibrium cell was computed by the formula (1):

$$n_{CO_2}^{Total} = \frac{P_0 \times V_t}{Z_0 \times R \times T} - \frac{P_1 \times V_t}{Z_1 \times R \times T} \quad (1)$$

where  $P_0$  is the initial pressure of the gas reservoir cell,  $P_1$  is the equilibrium pressure of the gas reservoir cell after the injection of the CO<sub>2</sub> into the equilibrium cell,  $T$  is the system temperature,  $V_t$  is the total volume of the gas reservoir cell plus the tubes connected to it, and  $R$  is the gas constant. The total CO<sub>2</sub> uptake amount ( $n_e$ ) in the equilibrium cell after absorption equilibrium was calculated using Eq. (2):

$$n_{CO_2}^{Equil} = \frac{P_E \times V_g}{Z_E \times R \times T} \quad (2)$$

where  $P_E$  is the equilibrium pressure of the equilibrium cell and  $Z_E$  is the compressibility factor corresponding to  $T$  and  $P_E$ .  $V_g$  is the volume of the equilibrium gas phase in the equilibrium cell after each experimental run. The total uptake of CO<sub>2</sub> in the absorbent was determined by formula (3):

$$n_{CO_2}^{Absorbed} = n_{CO_2}^{Total} - n_{CO_2}^{Equil} \quad (3)$$

The mass weight and molecular weight of the absorbent are known, so the molar solubility of CO<sub>2</sub> in absorbent ( $x_{CO_2}$ ) can be computed by Eq. (4):

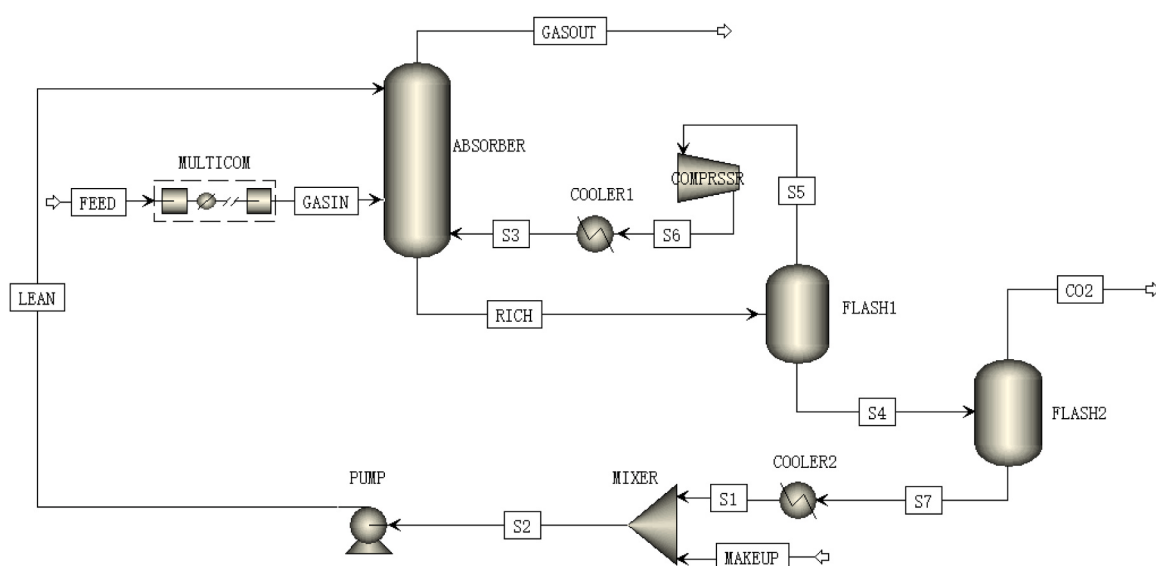
$$x_1 = \frac{n_{CO_2}}{n_{CO_2} + n_{Absorbent}} \quad (4)$$

In physical absorption process, the Henry's law constant based on mole fraction (Hx) can be determined by the following formula:

$$H_x(T, P) = \lim_{x_{CO_2} \rightarrow \infty} \frac{f_{CO_2}^L(T, P)}{x_{CO_2}} = \lim_{x_{CO_2} \rightarrow \infty} \frac{P\phi_{CO_2}(T, P)}{x_{CO_2}} = \frac{P_E}{x_{CO_2}} \quad (5)$$

where  $f_{CO_2}^L$  is the fugacity of CO<sub>2</sub>,  $\phi_{CO_2}$  is the fugacity coefficient, and  $P_E$  is the equilibrium pressure.  $f_{CO_2}^L$  is assumed to be equal to  $P_E$  under the moderate pressure range studied in this study. By correlating Henry's law constants, other important thermodynamic properties such as solution Gibbs free energy ( $\Delta_{sol}G$ ), solution enthalpy ( $\Delta_{sol}H$ ), and solution entropy ( $\Delta_{sol}S$ ) can be calculated by the following equations:

$$\Delta_{sol}G = RT \ln(H(T, P)) / p^0 \quad (6)$$

**Fig. 2.** Flow diagram of simulation.**Table 4**Estimated critical properties, density and viscosity of absorbent measured at 293.15 K temperature and  $p = 0.1$  MPa.

Solution	T <sub>c</sub> (K)	V <sub>c</sub> (cc/mol)	P <sub>c</sub> (bar)	$\omega$	Density (kg/m <sup>3</sup> )		Viscosity (cP)	
					Calculated	Experimental	Calculated	Experimental
SC/EG-20 wt%	465.53	201.83	78.98	0.50	1.12	1.16	15.23	15.92
CA/EG-20 wt%	458.69	213.55	77.68	0.49	1.11	1.08	29.65	30.21
PY/EG-20 wt%	459.50	202.26	78.87	0.50	1.14	1.09	19.44	20.07

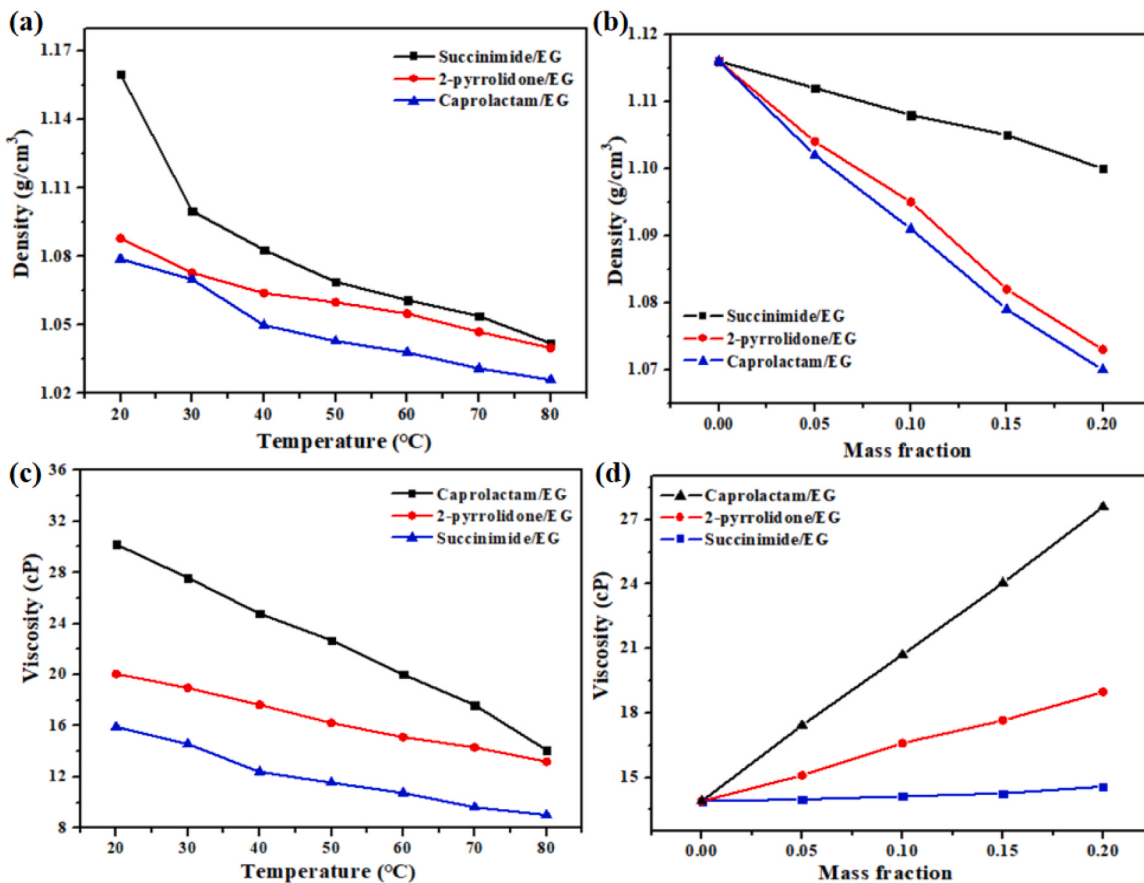


**Fig. 3.** (a) Density of the three imide-based/EG as a function of temperature; (b) Density of SC/EG-20 wt% as a function of SC loading; (c) Viscosity of the three imide-based/EG as a function of temperature; (d) Viscosity of SC/EG-20 wt% as a function of SC loading.

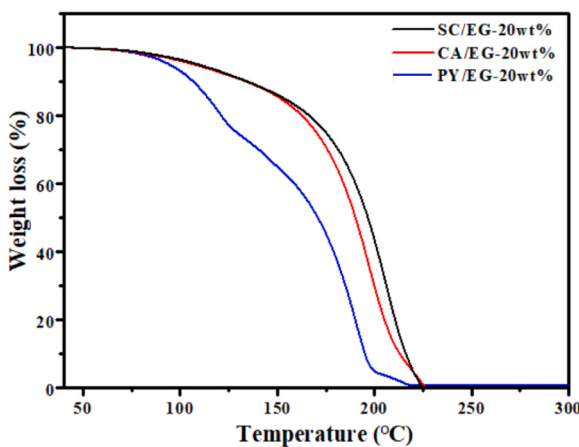


**Fig. 4.** Thermal stability of imide-based/EG measured using thermogravimetric analyzer under the nitrogen atmosphere.

$$\Delta_{sol}H = R \left( \frac{\partial \ln(H(T, P)) / p^0}{\partial (1/T)} \right)_P \quad (7)$$

$$\Delta_{sol}S = (\Delta_{sol}H - \Delta_{sol}G) / T \quad (8)$$

where  $p^0$  refers to the standard pressure of 0.1 MPa.

After  $\text{CO}_2$  capture, the  $\text{CO}_2$ -saturated absorbents were regenerated by heating combined with reduced pressure treatment. In a typical desorption of  $\text{CO}_2$ , using a vacuum pump to extract the absorbed gas from  $\text{CO}_2$ -saturated absorbents in a glass container, which was partly

immersed in a circulation oil bath, then slowly heat and heat it up. Under negative pressure conditions,  $\text{CO}_2$ -saturated absorbents can completely desorb within 30 minutes.

#### 2.4. The vapor-liquid equilibria modeling

The  $\text{CO}_2$  solubility in imide-based ethylene glycol absorbent are modeled by the Peng-Robinson equation, and the equation as follows:

$$p = \frac{RT}{v - b} - \frac{a}{v(v + b) + b(v - b)} \quad (9)$$

$$a = \sum_i \sum_j x_i x_j (a_i a_j)^{0.5} (1 - k_{ij}) \quad (10)$$

$$b = \sum_i x_i b_i \quad (11)$$

$$k_{ij} = k_{aij} + k_{bij} + k_{cij} \quad (12)$$

where  $k_{ij}$  is the temperature-dependent binary interaction parameter.

#### 2.5. Computational studies

All simulation and calculations for  $\text{CO}_2$  capture using imide compounds were carried out by the Gaussian 09 software package [33], and the most stable geometry has been fully optimized at the M06-2X/6-31 G\*\* level of theory.

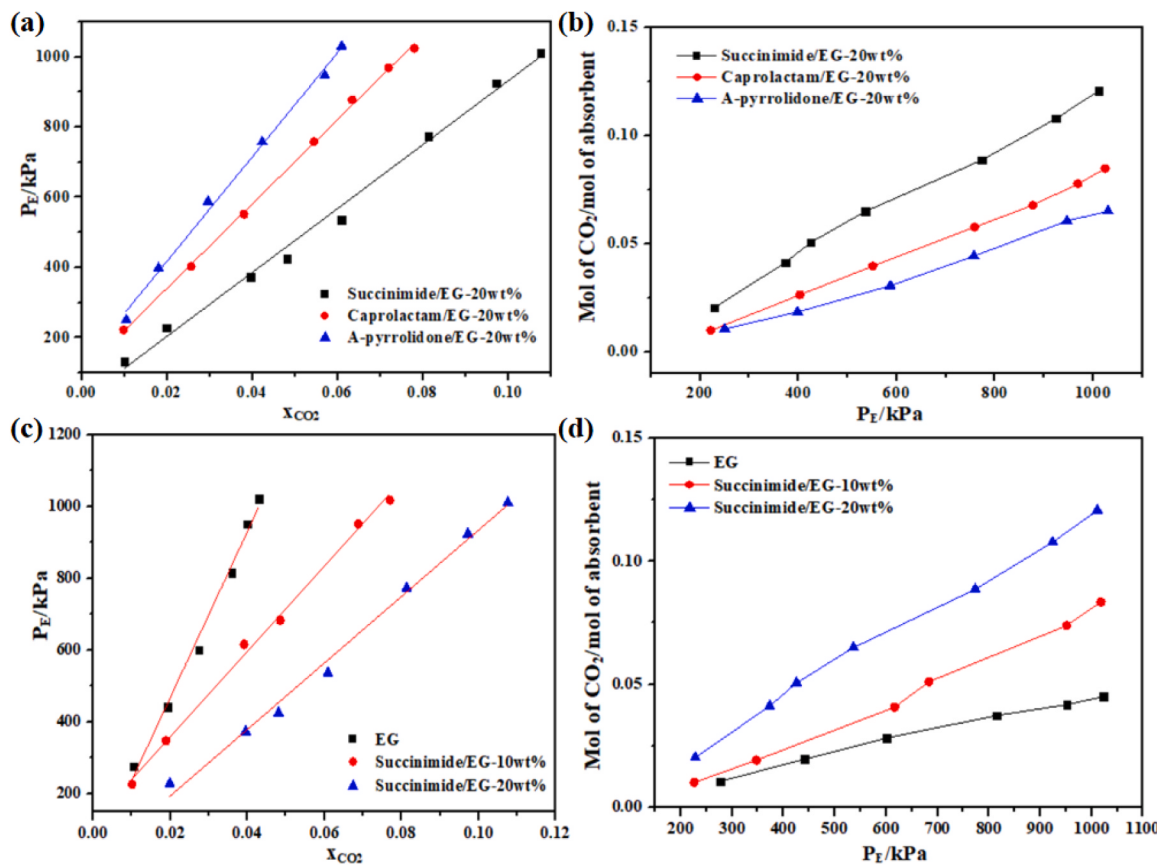


**Fig. 5.**  $\text{CO}_2$  solubility as a function of mole fraction (a) pressure (b) for the three imide-based/EG;  $\text{CO}_2$  solubility as a function of mole fraction (c) pressure (d) for different SC content of SC/EG absorbent.

## 2.6. Characterizations

A PerkinElmer Frontier spectrometer was used to record the FTIR spectrum of the absorbents before and after  $\text{CO}_2$  absorption. A Bruker spectrometer was applied to

record the  $^{13}\text{C}$  NMR (151 MHz) data using DMSO-d6 as the external reference. The thermogravimetric analysis (TGA) was conducted by Navas TGA-100 from 30 °C up to 900 °C under constant flow of helium.

## 2.7. Process modeling

Capturing carbon dioxide from flue gas was simulated using Aspen Plus (v.9.0) software [34]. The absorption tower was modeled using RADFRAC, and the flash tank selected the FLASH2. In addition, thermodynamic equilibrium was assumed on each tray of the absorption tower. The composition of carbon dioxide mixture was presented in Table 3, and the process flowsheet was designed in Fig. 2.

## 3. Results and discussion

### 3.1. Physical properties of different absorbents

Group contribution method was used to assess the critical properties of imide-based/EGs. The “Modified Lydersen-Joback-Reid” (LJR) method was employed to determine the individual properties of imide-based/EGs [35,36]. Furthermore, the critical performance of imide/EG was predicted using the Lee-Kesler’s mixing rules [37]. The critical properties of imide-based/EGs were estimated and the values are presented in Table 4. The estimated critical performance were used to compute the viscosity and density of imide-based EGs, which were well correlated with experimental values.

The densities and viscosities of imide-based/EG are firstly measured in the temperature range of 293.15–353.15 K. As shown in Fig. 3(a) and (c), for the three studied imide-based/EG at the same loading, the density and viscosity decreases linearly with the increase of temperature. For SC/EG absorbent, the density and viscosity increases with the increase of SC loading (see Figs. 3(a) and 3(c)). Viscosity plays to an extremely vital influence on the absorption process of  $\text{CO}_2$ . Higher viscosity affects mass transfer, while lower viscosity is beneficial for  $\text{CO}_2$  absorption. In general, the viscosity of the absorbent increases as the increase of SC, which means that SC plays a very important role in the viscosity. Obviously, although the viscosity of absorbent increased with SC addition, the viscosity value of SC/EG-20 wt% is still lower than most of reported literatures [38–40]. The SC/EG-20 wt% is employed as the representative for subsequent discussion, as it presents the best absorption performance as discussed later, and 20 wt% is maximum dissolution amount of SC in EG.

In order to understand the thermal stability of imide-based/EG fabricated in this study, the thermogravimetric analysis was conducted on the imide-based/EG absorbent, and the result of thermal stability was depicted in Fig. 4. It can be seen from Fig. 4 that SC/EG-20 wt% absorbent is more stable than CA/EG-20 wt% and PY/EG-20 wt% absorbents, which can be attributed to the higher bond strength between SC and EG in SC/EG-20 wt% absorbent.

### 3.2. Absorption performance of imide-based ethylene glycol absorbent

#### 3.2.1. The thermodynamics of absorption

The  $\text{CO}_2$  absorption performance of three imide-based ethylene glycol absorbent are depicted in Fig. 5. From the Fig. 5(a) and Fig. 5(b), it can be seen that  $\text{CO}_2$  absorption capacity of three absorbent follows the order of SC/EG-20 wt% > CA/EG-20 wt% > PY/EG-20 wt%, SC/EG-

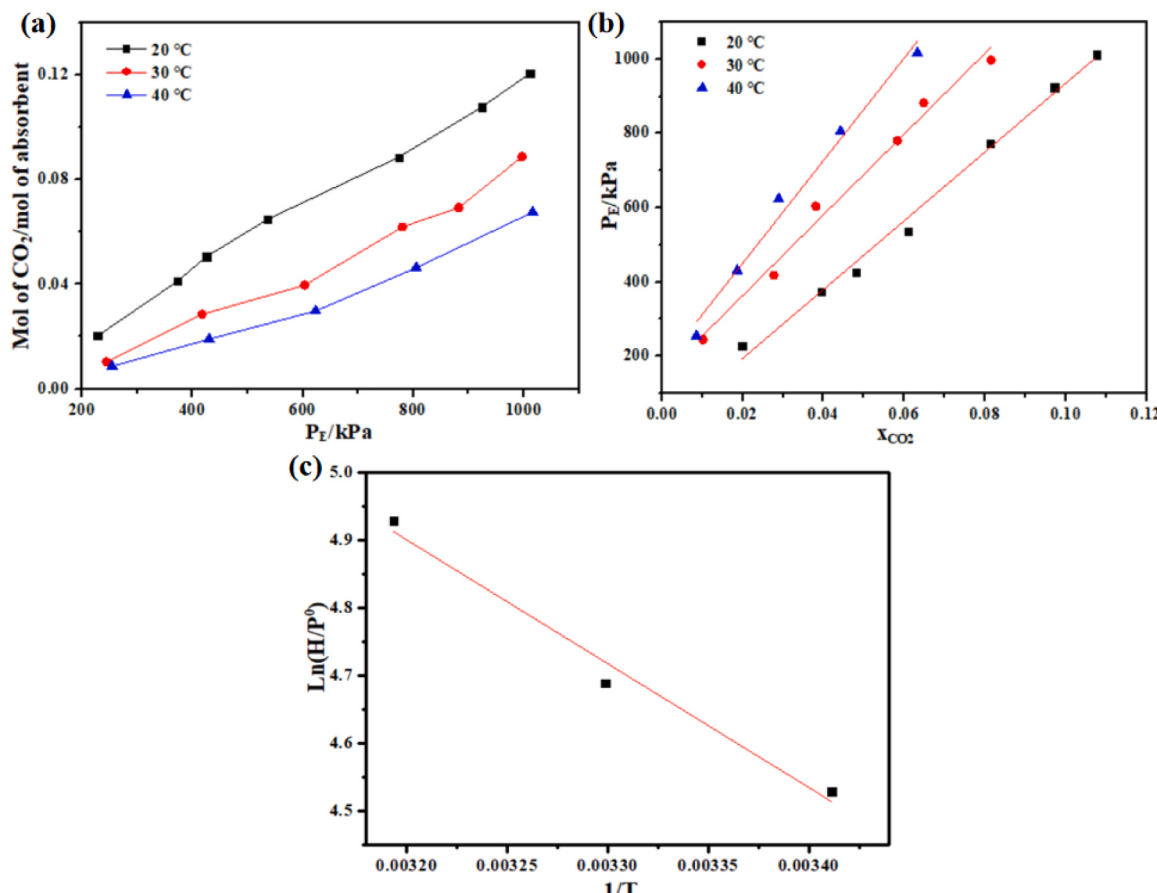


**Fig. 6.** CO<sub>2</sub> solubility of SC/EG-20 wt% absorbent at different temperature (20 °C, 30 °C, 40 °C) as a function of pressure with mole fraction (a) and molality (b); Variation of logarithm of Henry's constants (based upon mole fraction) SC/EG-20 wt% absorbent.

**Table 5**

Henry's Law Constants ( $H_x$ ) and Correlated Thermodynamic Properties of CO<sub>2</sub> in the Studied absorbents.

solution	Temperature	$H_x$ (MPa)	$\Delta_{\text{sol}}G$ (kJ/mol)	$\Delta_{\text{sol}}H$ (kJ/mol)	$\Delta_{\text{sol}}S$ (J·mol <sup>-1</sup> ·K <sup>-1</sup> )
SC/EG- 20 wt%	293.15	9.26	11.04	-15.22	-89.55
	303.15	10.88	11.82		-89.18
	313.15	13.82	12.83		-89.56

20 wt% could capture 0.97 mol CO<sub>2</sub> per mol SC/EG-20 wt% absorbent (0.085 g CO<sub>2</sub> per g SC/EG-20 wt% absorbent). However, the CO<sub>2</sub> solubility in CA/EG-20 wt% is as low as 0.01 mol CO<sub>2</sub> per mol CA/EG-20 wt% absorbent at 20 °C and 10 atm. The absorption capacity of PY/EG-20 wt% was also studied and it can only capture 0.68 mol CO<sub>2</sub> per mol PY/EG-20 wt% absorbent (0.069 g CO<sub>2</sub> per g PY/EG-20 wt% absorbent), which was much lower than that of SC/EG-20 wt%. The reason why SC/EG-20 wt% have maximum absorption capacity compared other two absorbents is one molecule of SC can absorb two molecules of carbon dioxide, while the other molecule of imide can only absorb one molecule of carbon dioxide, which will be clarified in detail in the mechanism section (see Section 3.4) and is consistent with the previously reported results [38].

It is well known that the mass content of amine has an significant impact on the CO<sub>2</sub> uptake, thus we carried out the absorption experiment of SC/EG absorbent with various mass fraction at 20 °C, were presented in Fig. 5(c) and Fig. 5(d). It can be observed that the CO<sub>2</sub> uptake order of SC/EG is the mass fraction of 20 % > 10 % > 0 %, the optimal SC/EG mass fraction for CO<sub>2</sub> absorption is 20 %. The higher

mass fraction of SC, the higher CO<sub>2</sub> absorption capacity, SC/EG-20 wt% have smallest Henry constant while having the highest solubility.

In the following, SC/EG-20 wt% absorbent is used to carry out the CO<sub>2</sub> absorption experiment. From the Fig. 6, it can be seen that the absorption of CO<sub>2</sub> varies inversely with the temperature, which is obvious from the decline in the slope with the rise of the temperature. This means that the fabricated SC/EG-20 wt% can be regenerated and recycled again at a higher temperature. In addition, as the pressure increases, the solubility of CO<sub>2</sub> also increases linearly. This trend typically occurs in other absorbents (such as ionic liquids and DESs) that capture CO<sub>2</sub> through physical absorption [39–41]. This experimental result is different from the previously reported non-aqueous amine solution system [24,42–45], which is believed to be chemical absorption, but our experimental results did not find any new bond formation after absorbing CO<sub>2</sub>, the physisorption behavior were confirmed by IR, <sup>13</sup>C and molecular simulation in the following mechanism analysis section (in Section 3.4).

The thermodynamic properties of SC/EG-20 wt% absorbent mutually related with the measured CO<sub>2</sub> solubility are tabulated in Table 5. For CO<sub>2</sub> absorption process in the SC/EG-20 wt% absorbent, the positive values of  $\Delta_{\text{sol}}G$  indicates that the CO<sub>2</sub> absorption for SC/EG-20 wt% absorbent is a non-spontaneous process. The negative  $\Delta_{\text{sol}}H$  implies that the CO<sub>2</sub> absorption process for SC/EG-20 wt% absorbent is exothermic. Compared with ordinary organic solvents, the smaller absolute values (e.g., -85 kJ·mol<sup>-1</sup> for CO<sub>2</sub> in MDEA) suggest that SC/EG-20 wt% absorbents are more easily regenerated [46]. The larger negative  $\Delta_{\text{sol}}S$ , the higher ordering degree of the absorbent after CO<sub>2</sub> absorption.

### 3.2.2. The kinetics of absorption

It is well known that species of amine also has an significant impact

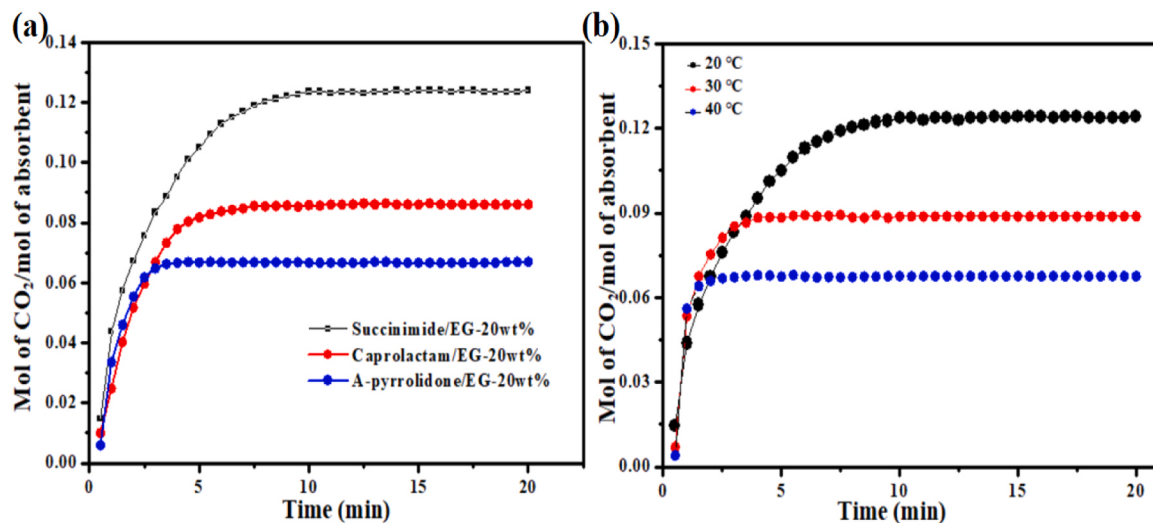


Fig. 7.  $\text{CO}_2$  uptake kinetics in (a) the three absorbent at 293.15 K; (b) the three different temperature in SC/EG-20 wt% absorbent.

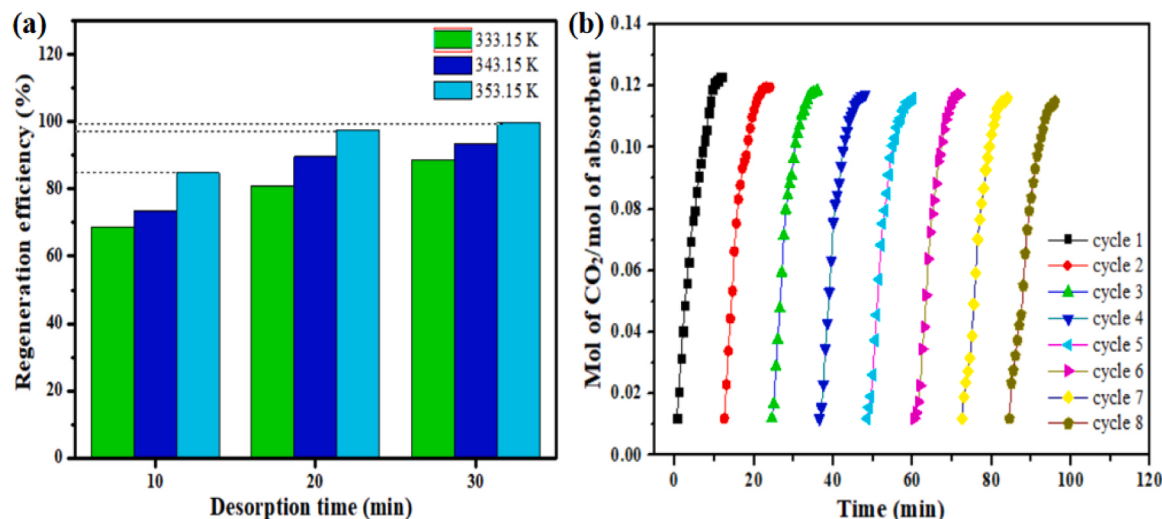


Fig. 8. Desorption performance of SC/EG-20 wt% absorbent. (a) Effect of desorption temperature and time on the regeneration efficiency and (b) Recyclability at 353.15 K for 30 min.

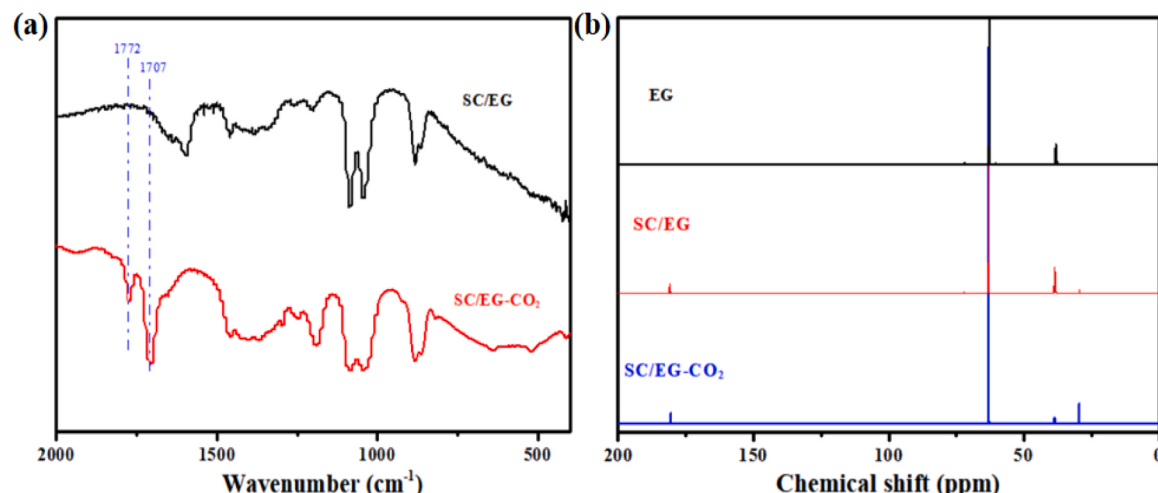
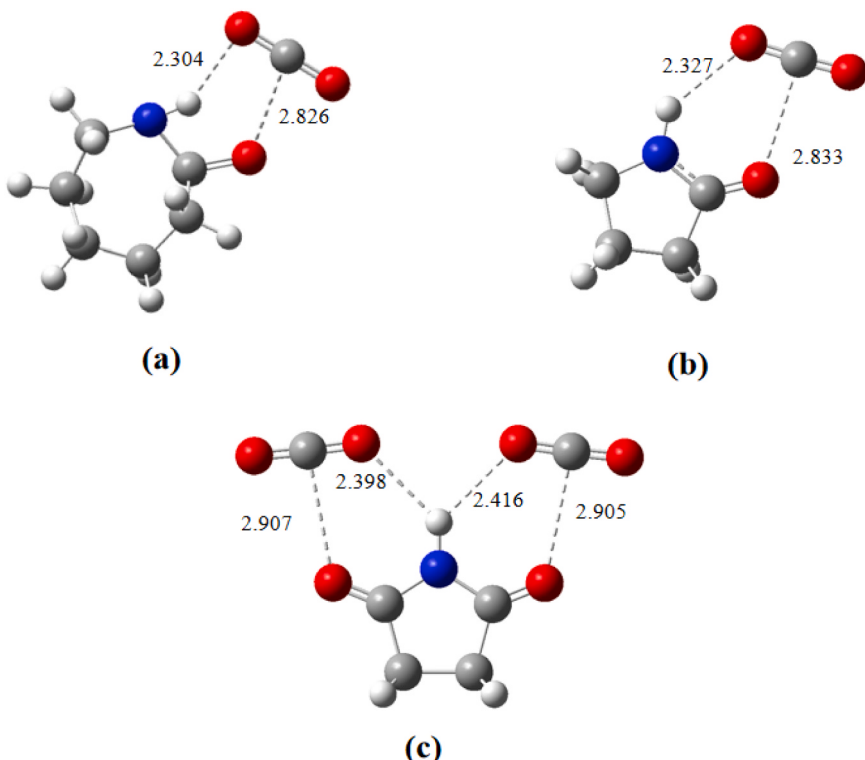


Fig. 9. (a)FT-IR spectra of SC/EG-20 wt% absorbent before and after the absorption of  $\text{CO}_2$  at 20 °C and 10 bar; (b)  $^{13}\text{C}$  NMR spectra of EG, SC/EG and SC/EG- $\text{CO}_2$  at 20 °C and 10 bar.



**Fig. 10.** Optimized structures of SC- $\text{CO}_2$ . Note that van der Waals radii (in Å) are 1.70 (C), 1.20 (H), 1.52 (O), and 1.55 (N), respectively. O, red; N, blue; C, gray; H, white.

**Table 6**  
Comparison of  $\text{CO}_2$  solubility of various solvents reported in the literature.

Solvents	T (K)	P (bar)	$\text{CO}_2$ uptake (mol $\text{CO}_2$ /mol solvent)	Ref.
SC/EG	293.15	10.11	0.121	This work
MTPPhBr/4EG	303.15	10.19	0.053	[47]
MTPPhBr/ 4DEG	303.15	09.21	0.062	[47]
MTPPhBr/ 3GLY	303.15	10.39	0.059	[47]
MTPPhBr/6EA	298.15	10.00	0.140	[48]
TBAB/6EA	298.15	10.00	0.120	[48]
ChCl/6EA	298.15	10.00	0.109	[48]
BTPPhBr/ 12EG	298.15	10.00	0.050	[48]
ChCl/3Gly	298.15	10.00	0.045	[48]
ChCl/4EG	298.15	10.00	0.023	[48]
4TBAB/4EAE	303.15	09.93	0.220	[49]
GUA/2EA	298.15	11.29	0.019	[50]
TPAC/4EA	298.15	10.57	0.009	[50]
TEMA/2EG	298.15	10.41	0.007	[50]
TEMA/2GLY	298.15	12.38	0.003	[50]
ChCl/4DEG	303.15	09.24	0.0308	[51]
TBAB/4EG	303.15	10.45	0.0386	[51]
TBAB/4DEG	303.15	10.48	0.0985	[51]

on the  $\text{CO}_2$  uptake kinetics of non-aqueous solution, so  $\text{CO}_2$  uptake kinetics were explored with three imide-based/EG at 10 bar, as depicted in Fig. 7(a). It can be seen that the absorption rate of the three imide-based ethylene glycol absorbents gradually declined until they

reached a steady state, and the time for the three absorbents to reach equilibrium is about 10 minutes for SC/EG-20 wt%, 7 minutes for CA/EG-20 wt%, and 3 minutes for PY/EG-20 wt%, respectively. It can be clearly observed that the absorption rate follows the order of SC/EG-20 wt% > PY/EG-20 wt% > CA/EG-20 wt%, the absorption rate of SC/EG-20 wt% absorbent is the highest because of the low viscosity. We also notice in Fig. 7(b) that as the arise of temperature, the absorption equilibrium is achieved sooner, but this comes at the cost of the absorption amount. The result indicated that the viscosity of SC/EG-20 wt % becomes larger and the hydrogen bond network between SC and EG or EG and EG becomes denser with the decrease of temperature, which might hinder the intermolecular force between SC and  $\text{CO}_2$ . As the

**Table 8**  
Simulation results of process.

	GASOUT	S4	S5	S7	$\text{CO}_2$
Temperature/K	292.96	273.15	273.15	273.15	353.15
Pressure/MPa	0.15	0.1	0.1	0.1	0.01
Mole Flows/ $\text{kmol}\cdot\text{h}^{-1}$	849.295	11149.116	2.607	10999.304	149.817
$\text{CO}_2/\text{kmol}\cdot\text{h}^{-1}$	1.189	113.721	1.469	2.530	149.427
$\text{N}_2/\text{kmol}\cdot\text{h}^{-1}$	848.021	0.114	0.641	0.0000688	0.165
SC/EG-20 wt%	0.074	11035.395	0.00005	10997.104	0.047
Mole Fractions					
$\text{CO}_2$	0.0014	0.0102	0.5633	0.00023	0.9988
$\text{N}_2$	0.9985	1.0188E-05	0.4366	6.256E-09	0.0011
SC/EG-20 wt%	8.760e-05	0.9898	1.985E-05	0.9998	3.162E-04

**Table 7**  
Estimated Peng-Robinson binary parameters.

Component i	Component j	$k_{\text{Aij}}$	$k_{\text{Bij}}$	$k_{\text{Cij}}$	$T_{\text{lower(K)}}$	$T_{\text{upper(K)}}$
SC/EG-20 wt%	$\text{CO}_2$	-14.22	-0.00048	110000	-5.1159e-13	1000

**Table 9**  
Key parameters for process.

	Power consumption/ kW·h·(t CO <sub>2</sub> ) <sup>-1</sup>	Cold utility consumption/GJ·(t CO <sub>2</sub> ) <sup>-1</sup>	Regeneration duty/ GJ·(t CO <sub>2</sub> ) <sup>-1</sup>
SC/EG- 20 wt %	623.06	-2.58	2.243

**Table 10**  
Power requirement of the conceptual process.

Equipment	Consumption/MW
Multi-stage compressor	13.085
Compressor	0.073
Circulating pump	0.894
Total power consumption	14.052

temperature increases, hydrogen bond network becomes weaker, which is conducive to the absorption of CO<sub>2</sub>.

### 3.3. Absorption-desorption cycle performance of SC/EG-20 wt% absorbent

In order to ultimately achieve the industrial application, the absorption- desorption performances also have been studied. After absorption equilibrium, the CO<sub>2</sub> saturated absorbent was desorbed via heating at negative pressure (-0.1 MPa). The influence of desorption time and desorption temperature on the regeneration ratio were studied. As seen from Fig. 8(a), the regeneration ratio increased with the arise of desorption temperature and desorption time. When the desorption temperature varied from 333.15 to 353.15 K, the regeneration ratio of the absorbent reached more than 85.0 %, they increased under different desorption time by 21.7 %, 22.5 %, and 12.5 %, respectively. When extending the desorption time from 15 min to 30 min, the regeneration ratio at different desorption temperatures increased by 27.5 %, 23.0 %, and 16.5 %, respectively. It can be seen that increasing the desorption temperature or extending the desorption time will enhance the regeneration ratio. When the absorbent was desorbed at 353.15 K for 30 min, the regeneration ratio up to 99.7 %, which implied that the saturated SC/EG-20 wt% absorbent was almost completely desorbed. Furthermore, the regeneration ratio was 97.9 % and only decreased by 1.8 % when the desorption time reduced to 20 min, the absorbent still retained a high regeneration ratio. In order to investigate the recyclability from the perspective of economy and energy, the absorbent was desorbed under the condition of 353.15 K and 30 min, and the recycle results are presented in Fig. 8(b). SC/EG-20 wt% absorbent still retained its high regeneration ratio of 96.2 % after the eighth cycle, and it was better than reported MEA aqueous solution, which only has a regeneration ratio of 88.1 % after the first cycle [46].

### 3.4. CO<sub>2</sub> capture mechanism

To understand the CO<sub>2</sub> capture mechanism of SC/EG-20 wt% absorbent, the microscopic behaviors of {SC/EG-20 wt% absorbent + CO<sub>2</sub>} systems are further investigated. Fig. 9(a) clearly presents the peak change in the absorption of CO<sub>2</sub> (based on mol CO<sub>2</sub> per mol SC/EG-20 wt%). After CO<sub>2</sub> was captured by SC/EG-20 wt%, a characteristic peak at 1772 cm<sup>-1</sup> and 1707 cm<sup>-1</sup> could be ascribed to the asymmetric C=O vibration in NH···CO<sub>2</sub> and C=O···CO<sub>2</sub>, respectively. Fig. 10 shows the molecular simulation (MS) results of amide compounds absorbing carbon dioxide molecules. From the molecular simulation results, it can be seen that amide molecules absorb carbon dioxide molecules through intermolecular hydrogen bonds and van der Waals forces. Moreover, due to the presence of two carbon groups in the molecule, one

succinimide molecule can theoretically absorb two carbon dioxide molecules, which is why the absorption capacity of succinimide is better than that of the other two amide compounds. Such the calculation results of molecular simulation can be confirmed via the <sup>13</sup>C nuclear magnetic resonance (NMR) spectroscopy before and after CO<sub>2</sub> absorption by SC/EG-20 wt% absorbent (Fig. 9(b)). For instance, the <sup>13</sup>C NMR spectrum of CO<sub>2</sub>-absorbed SC/EG-20 wt% absorbent is the same as that of fresh SC/EG-20 wt% absorbent, where no new chemical shift peak is found in the <sup>13</sup>C NMR spectroscopy (see Fig. 9(b)). The research results suggest that CO<sub>2</sub> are physically absorbed by the SC/EG-20 wt% absorbent.

### 3.5. Comparison of CO<sub>2</sub> capture performance with reported absorbent

In order to further assess the CO<sub>2</sub> absorption performance of SC/EG absorbent, the CO<sub>2</sub> capture capacity of SC/EG absorbent in this study was compared with other absorbents (Table 6). It is obvious that CO<sub>2</sub> capture capacity of SC/EG is more competitive than most of the absorbents, which indicated that SC/EG system as CO<sub>2</sub> absorbent exhibit the enormous advantages for capturing CO<sub>2</sub>.

### 3.6. Simulation of SC/EG-20 wt% absorbent decarbonization process

The VLE experimental data using the PR-EOS to model for the CO<sub>2</sub>-SC/EG-20 wt% absorbent. The experimental data of SC/EG-20 wt% absorbent was regressed and the regressed coefficient are listed in Table 7.

The design requirements are as follows: CO<sub>2</sub> mole purity is higher than 99.8 %, and the process simulation results are shown in Tables 8–10. Compared with the conventional amine solution absorbent capture, the imide-based ethylene glycol system absorbing CO<sub>2</sub> suggested in this study consumes much various forms of energy. The conventional process consumes mainly heat energy, while the process of the imide-based ethylene glycol system, mainly consumes electric energy. The energy consumption of SC/EG-20 wt% absorbent is only consumed 2.243 GJ·(t CO<sub>2</sub>)<sup>-1</sup> of electric energy, and cold utility consumption is -2.58 GJ/t (CO<sub>2</sub>). The power consumption of equipment is presented in Table 10. From Table 10, the power consumption of the whole process is 14.052 MW. The compression consumption of carbon dioxide mixture accounts for a large proportion (about 93.12 %) in the total power consumption.

## 4. Conclusion

In summary, three imide-based ethylene glycol system absorbents, namely, SC/EG, CA/EG, and PY/EG, are fabricated, and their CO<sub>2</sub> solubility are measured. The SC/EG-20 wt% absorbent have a competitive CO<sub>2</sub> solubility compared with the reported absorbents. The absorption mechanism of CO<sub>2</sub> is confirmed by the IR and <sup>13</sup>C spectrum of {SC/EG-20 wt% absorbent + CO<sub>2</sub>} systems, the absorption of CO<sub>2</sub> did not cause any structural changes in the SC/EG-20 wt% absorbent, which could be mainly ascribed to the strong hydrogen bond interactions or Van der Waals force between CO<sub>2</sub> and imide. Additionally, after eight cycles, the CO<sub>2</sub> absorption performance of the SC/EG-20 wt% absorbent decreased slightly. Last, the process simulation results suggest that the energy consumption of regeneration is only 2.243 GJ/t (CO<sub>2</sub>). This indicates that SC/EG-20 wt% can be used as a potential absorbent for CO<sub>2</sub>.

### CRediT authorship contribution statement

**yong pan:** Writing – original draft, Investigation. **Wei Huang:** Methodology, Investigation. **Dengyi Ma:** Formal analysis, Data curation. **Qiaoqiao Tang:** Resources, Conceptualization. **Bo Sun:** Writing – review & editing, Supervision. **BaoMing Xu:** Validation.

## Declaration of Competing Interest

The authors declare that they have no known competing financial interests or personal relationships that could have appeared to influence the work reported in this paper.

## Data availability

The data that has been used is confidential.

## Acknowledgements

This research was funded by the Startup Foundation of Hubei University of Technology (grant number BSQD2020029) and Open Project of Key Laboratory of Green Chemical Engineering Process of Ministry of Education.

## References

- [1] O. Isabelle, C. Thiago, F. Larissa, T. Luciano, G. Rodolfo, M. Ronconi, M. Walkimar, Combined theoretical and experimental studies on CO<sub>2</sub> capture by amine-activated glycerol, *Chem. Eng. J.* 408 (2021) 128002.
- [2] T. Wang, A.M. Gaffney, D.J. Heldebrant, Editorial: rising stars in carbon capture, utilization and storage: 2022, *Front. Energy Res.* 11 (2023) 1167769.
- [3] N.N. Dalei, J. Joshi, Potential matching of carbon capture storage and utilization (CCUS) as enhanced oil recovery in perspective to Indian oil refineries, *Clean. Technol. Environ.* 24 (2022) 2701–2717.
- [4] F. Raganati, F. Miccio, P. Ammendola, Adsorption of carbon dioxide for post-combustion capture: a review, *Energ. Fuel.* 35 (2021) 12845–12868.
- [5] B. David, N. Petter, A. Rahul, Low-temperature CO<sub>2</sub> removal from natural gas, *Energ. Procedia* 26 (2012) 41–48.
- [6] Y. Wang, Z. Pan, W.X. Zhang, S.C. Huang, G.J. Yu, M.R. Soltanian, E. Lichtfouse, Z. E. Zhang, Higher efficiency and lower environmental impact of membrane separation for carbon dioxide capture in coal power plants, *Environ. Chem. Lett.* 21 (2023) 1951–1958.
- [7] M. Hosseinpour, M.J. Shojaei, M. Salimi, M. Amidpour, Machine learning in absorption-based post-combustion carbon capture systems: a state-of-the-art review, *Fuel* 353 (2023) 129265.
- [8] M. Castro, D. Gómez-Díaz, J.M. Navaza, A. Rumbo, Carbon dioxide capture by chemical solvents based on amino acids: absorption and regeneration, *Chem. Eng. Technol.* 44 (2020) 248–257.
- [9] A. Baltar, D. Gómez-Díaz, J.M. Navaza, A. Rumbo, Absorption and regeneration studies of chemical solvents based on dimethylethanolamine and diethylethanolamine for carbon dioxide capture, *AIChE J.* 66 (1) (2020) e16770.
- [10] H. Isogai, T. Nakagaki, Mechanistic analysis of post-combustion CO<sub>2</sub> capture performance during amine degradation, *Int. J. Green. Gas. Con.* 114 (2022) 103597.
- [11] I.M. Saeed, V.S. Lee, S.A. Mazari, B.S. Ali, W.J. Basirun, A. Asghar, L. Ghaleb, B. M. Jan, Thermal degradation of aqueous 2-aminoethylethanolamine in CO<sub>2</sub> capture; identification of degradation products, reaction mechanisms and computational studies, *Chem. Cent. J.* 11 (2017) 132–145.
- [12] Y. Pan, H. Li, X.X. Zhang, Z. Zhang, X.S. Tong, C.Z. Jia, B. Liu, C.Y. Sun, L.Y. Yang, G.J. Chen, Large-scale synthesis of ZIF-67 and highly efficient carbon capture using a ZIF-67/glycol-2-methylimidazole slurry, *Chem. Eng. Sci.* 137 (2015) 504–514.
- [13] Q.H. Lai, L.L. Kong, W.B. Gong, Armistead G. Russell, M.H. Fan, Low-energy-consumption and environmentally friendly CO<sub>2</sub> capture via blending alcohols into amine solution, *Appl. Energ.* 254 (2019) 113696.
- [14] W. Conway, S. Bruggink, Y. Beyad, W. Luo, I. Melián-Cabrera, G. Puxty, P. Feron, CO<sub>2</sub> absorption into aqueous amine blended solutions containing monoethanolamine (MEA), N,N-dimethylethanolamine (DMEA), N,N-diethylethanolamine (DEEA) and 2-amino-2-methyl-1-propanol (AMP) for post-combustion capture processes, *Chem. Eng. Sci.* 126 (14) (2015) 446–454.
- [15] M.I. Habibullah, A. Veawab, Cysteine as an alternative eco-friendly corrosion inhibitor for absorption-based carbon capture, *Plants. Mater.* 16 (2023) 3496.
- [16] T.T. Ping, Y. Dong, S.F. Shen, Energy-efficient CO<sub>2</sub> capture using nonaqueous absorbents of secondary alkanolamines with a 2-butoxyethanol cosolvent, *ACS Sustain. Chem. Eng.* 8 (2020) 18071–18082.
- [17] H. Guo, C.X. Li, X.Q. Shi, H. Li, S.F. Shen, Nonaqueous amine-based absorbents for energy efficient CO<sub>2</sub> capture, *Appl. Energ.* 239 (2019) 725–734.
- [18] H. Guo, L. Hui, S. Shen, Monoethanolamine<sup>+</sup> 2-methoxyethanol mixtures for CO<sub>2</sub> capture: density, viscosity and CO<sub>2</sub> solubility, *J. Chem. Thermodyn.* 132 (2019) 155–163.
- [19] S.W. Chai, L.H. Ngu, B.S. How, Review of carbon capture absorbents for CO<sub>2</sub> utilization, *Greenh. Gases.* 12 (2022) 394–427.
- [20] S. Chen, S. Chen, Y. Zhang, H. Chai, L. Qin, Y. Gong, An investigation of the role of N-methyl-diethanolamine in non-aqueous solution for CO<sub>2</sub> capture process using <sup>13</sup>C NMR spectroscopy, *Int. J. Greenh. Gas. Control.* 39 (2015) 166–173.
- [21] C. Zheng, J. Tan, Y.J. Wang, G.S. Luo, CO<sub>2</sub> solubility in a mixture absorption system of 2-amino-2-methyl-1-propanol with ethylene glycol, *Ind. Eng. Chem. Res.* 52 (2013) 12247–12252.
- [22] B.H. Lv, K.X. Yang, X.B. Zhou, Z.M. Zhou, G.H. Jing, 2-Amino-2-methyl-1-propanol based non-aqueous absorbent for energy-efficient and non-corrosive carbon dioxide capture, *Appl. Energ.* 264 (2020) 114703.
- [23] F. Liu, G. Jing, X. Zhou, B. Lv, Z. Zhou, Performance and mechanisms of triethylene tetramine (TETA) and 2-amino-2-methyl-1-propanol (AMP) in aqueous and nonaqueous solutions for CO<sub>2</sub> capture, *ACS Sustain. Chem. Eng.* 6 (2018) 1352–1361.
- [24] F. Barzagli, C. Giorgi, F. Mani, M. Peruzzini, Reversible carbon dioxide capture by aqueous and non-aqueous amine-based absorbents: a comparative analysis carried out by <sup>13</sup>C NMR spectroscopy, *Appl. Energ.* 220 (2018) 208–219.
- [25] K.S. Hwang, S.W. Park, D.W. Park, S.S. Kim, Absorption of carbon dioxide into diisopropanolamine solutions of polar organic solvents, *J. Taiwan. Inst. Chem. Eng.* 41 (2010) 16–21.
- [26] W. Tian, K. Ma, J.Y. Ji, S.Y. Tang, S. Zhong, C.J. Liu, H.R. Yue, B. Liang, Nonaqueous MEA/PEG200 absorbent with high efficiency and low energy consumption for CO<sub>2</sub> capture, *Ind. Eng. Chem. Res.* 60 (2021) 3871–3880.
- [27] F. Barzagli, C. Giorgi, F. Mani, M. Peruzzini, Comparative study of CO<sub>2</sub> capture by aqueous and nonaqueous 2-amino-2-methyl-1-propanol based absorbents carried out by <sup>13</sup>C NMR and enthalpy analysis, *Ind. Eng. Chem. Res.* 58 (2019) 4364–4373.
- [28] F. Almomani, M. Tawalbeh, A.A. Othman, R. Martis, K. Rasool, Current status of CO<sub>2</sub> capture with ionic liquids: development and progress, *Fuel* 344 (2023) 128102.
- [29] D. Hospital-Benito, C. Moya, M. Gazzani, J. Palomar, Direct air capture based on ionic liquids: From molecular design to process assessment, *Chem. Eng. J.* 468 (2023) 143630.
- [30] D.Z. Yang, M. Lv, J. Chen, Efficient non-aqueous solvent formed by 2-piperidinethanol and ethylene glycol for CO<sub>2</sub> absorption, *Chem. Commun.* 55 (2019) 12483.
- [31] H. Liu, B. Liu, L.C. Lin, G.J. Chen, Y.Q. Wu, J. Wang, X.T. Gao, Y.N. Lv, Y. Pan, X. X. Zhang, L.Y. Yang, C.Y. Sun, B. Smit, W.C. Wang, A hybrid absorption-adsorption method to efficiently capture carbon, *Nat. Commun.* 5 (2014) 5147.
- [32] Y. Pan, H. Li, X.X. Zhang, Z. Zhang, X.S. Tong, C.Z. Jia, B. Liu, C.Y. Sun, L.Y. Yang, G.J. Chen, Large-scale synthesis of ZIF-67 and highly efficient carbon capture using a ZIF-67/glycol-2-methylimidazole slurry, *Chem. Eng. Sci.* 137 (2015) 504–514.
- [33] M.J. Frisch, G.W. Trucks, H.B. Schlegel, G.E. Scuseria, M.A. Robb, J.R. Cheeseman, G. Scalmani, V. Barone, B. Mennucci, G.A. Petersson, Gaussian 09, Revision D.01; Revision B.01, Gaussian, Inc., Wallingford CT (2010).
- [34] ASPEN P.L.U.S. 2013-Aspen Plus, Aspen Technology, Inc., USA, 2018.
- [35] J.O. Valderrama, L.A. Forero, R.E. Rojas, Critical properties and normal boiling temperature of ionic liquids. Update and a new consistency test, *Ind. Eng. Chem. Res.* 51 (2012) 7838–7844.
- [36] J.O. Valderrama, W.W. Sanga, J.A. Lazzús, Critical properties, normal boiling temperatures andacentric factors of another 200 ionic liquids, *Ind. Eng. Chem. Res.* 47 (2008) 1318–1330.
- [37] S.D. Labinov, J.R. Sand, An analytical method of predicting Lee-Kesler-Ploeger equation-of-state binary interaction coefficients, *Int. J. Thermophys.* 16 (1995) 1393–1411.
- [38] Y.J. Huang, G.K. Cui, Y.L. Zhao, H.Y. Wang, Z.Y. Li, S. Dai, J.J. Wang, Preorganization and cooperation for highly efficient and reversible capture of low-concentration CO<sub>2</sub> by ionic liquids, *Angew. Chem. Int. Ed.* 56 (2017) 13293–13297.
- [39] M.B. Haider, P. Maheshwari, R. Kumar, CO<sub>2</sub> capture from flue gas using phosphonium based deep eutectic solvents: modeling and simulation approach, *J. Environ. Chem. Eng.* 9 (2021) 106727.
- [40] H. Qin, Z. Song, H.Y. Cheng, L.Y. Deng, Z.W. Qi, Physical absorption of carbon dioxide in imidazole-PTSA based deep eutectic solvents, *J. Mol. Liq.* 326 (2021) 115292.
- [41] J.W. Wang, H.Y. Cheng, Z. Song, L.F. Chen, L.Y. Deng, Z.W. Qi, Carbon dioxide solubility in phosphonium-based deep eutectic solvents: an experimental and molecular dynamics study, *Ind. Eng. Chem. Res.* 58 (2019), 175145–17523.
- [42] I.O. Furtado, T.C. dos Santos, L.F. Vasconcelos, L.T. Costa, R.G. Fiorot, C. M. Ronconi, J. Walkimar, de, M. Carneiro, Combined theoretical and experimental studies on CO<sub>2</sub> capture by amine-activated glycerol, *Chem. Eng. J.* 408 (2021) 128002.
- [43] H.N. Sang, L. Su, W.F. Han, F. Si, W.H. Yue, X.M. Zhou, Z.H. Peng, H. Fu, Basicity-controlled DBN-based deep eutectic solvents for efficient carbon dioxide capture, *J. CO<sub>2</sub> Util.* 65 (2022) 102201.
- [44] T.T. Ping, Y. Dong, S.F. Shen, Energy-efficient CO<sub>2</sub> capture using nonaqueous absorbents of secondary alkanolamines with a 2-butoxyethanol cosolvent, *ACS Sustain. Chem. Eng.* 8 (2020) 18071–18082.
- [45] D. Peng, J. Zhang, H. Cheng, L. Chen, Z. Qi, Computer-aided ionic liquid design for separation processes based on group contribution method and COSMO-SAC model, *Chem. Eng. Sci.* 159 (2017) 58–68.
- [46] A.A. Khan, G.N. Halder, A.K. Saha, Comparing CO<sub>2</sub> removal characteristics of aqueous solutions of monoethanolamine, 2-amino-2-methyl-1-propanol, methyldiethanolamine and piperazine through absorption process, *Int. J. Greenh. Gas. Con.* 50 (2016) 179–189.
- [47] M.B. Haider, P. Maheshwari, R. Kumar, CO<sub>2</sub> capture from flue gas using phosphonium based deep eutectic solvents: modeling and simulation approach, *J. Environ. Chem. Eng.* 9 (2021) 106727.
- [48] E. Ali, M.K. Kali, S. Mulyono, I. Alnashef, A. Fakieha, F. Mjallia, A. Hayyan, Solubility of CO<sub>2</sub> in deep eutectic solvents: experiments and modeling using the Peng-Robinsoninson equation of state, *Chem. Eng. Res. Des.* 92 (2014) 1898–1906.

- [49] M.B. Haider, R. Kumar, Solubility of CO<sub>2</sub> and CH<sub>4</sub> in sterically hindered aminebased deep eutectic solvents, *Sep. Purif. Technol.* 248 (2020) 117055.
- [50] S. Sarmad, Y. Xie, J.P. Mikkola, X. Ji, Screening of deep eutectic solvents (DESs) as green CO<sub>2</sub> sorbents: from solubility to viscosity, *N. J. Chem.* 41 (2017) 290–301.
- [51] M.B. Haider, D. Jha, B.M. Sivagnanam, R. Kumar, Thermodynamic and kinetic studies of CO<sub>2</sub> capture by glycol and amine-based deep eutectic solvents, *J. Chem. Eng. Data.* 63 (2018) 2671–2680.